Elastic model of composite sandwich structure model with progressive damage for low-velocity impact

T. Mandys [1a], V. Laš [1], T. Kroupa [1], C. Štádler [2], J. Bartošek [3]

[1] *University of West Bohemia in Pilsen, NTIS - New Technologies for Information Society, European Centre of Excellence, Univerzitní 8, 306 14 Pilsen, Czech Republic*

[2] *University of West Bohemia in Pilsen, Faculty of Mechanical Engineering, The Research Centre of Forming Technology - FORTECH, Univerzitní 8, 306 14 Pilsen, Czech Republic*

[3] *University of West Bohemia in Pilsen, Faculty of Applied Sciences, Department of Mechanics, Univerzitní 8, 306 14 Pilsen, Czech Republic*

[a] *tmandys@ntis.zcu.cz*

Abstract: This paper is focused on progressive failure analysis of sandwich composite beam loaded with transversely low-velocity impact. A user defined material model was used for modeling of the non-linear elastic behavior of composite skin of resulted sandwich structure. The non-linear behavior of foam core was modeled using Low-Density Foam material model. The results between numerical model and performed experiments were compared in form of deflection and contact force time dependencies and occurrence of damage too.

Keywords: Drop tester; Low-velocity impact; Sandwich structure, Fiber glass textile composite, Polymer foam core.

1 Introduction

Sandwich structures offer great potential for use in aerospace, marine and transportation and other low-bearing engineering, where the weight must be keep for any reason to a minimum value. Sandwich structure is built by two face sheets (skins) and light core. The outer skins are obviously thinner than the core. The main purpose of the core is to maintain the distance between stiffer outer skins and to transfer the shear load while skins carry compressive and tensile load. This structural arrangement have much larger bending stiffness than single solid plate made of the same total weight from the same material as outer skin only. The other benefits of sandwich panels are the excellent thermal insulation, acoustic damping, easy machining, etc. However, these sandwich panels have usually very low damage resistance and are susceptible to impact damage. The prediction and the prevention of the panel's impact damage are important in design of these panels and their applications. The sandwich structures may be subjected to randomly low-velocity impacts in every day life application such as dropped tool during repair, hit by a stone, or fall of different objects as cell phones. These low-velocity, or low-energy impacts, can cause damage on the sandwich structure that cannot be visible by naked eye, but may significantly reduce the residual strength or stiffness and affect the lifetime of structure or safety of the whole construction. In practice damage can be detected using CT-scan [1] or using structural health monitoring (SHM) [2] based on piezoelectric sensors [3]. These damage detection processes are very time-consuming and expensive. Therefore, it is necessary to ensure the safety of sandwich structures in all cases of expected loads and expected random impact loads.

Even though the non-linear behavior of composite materials is most evident in case of in-plane shear tests [4] the most reported works devoted to numerical simulations of low-velocity impacts consider the composite skin of sandwich structure as a linear orthotropic material. The experimental testing shows, that the fiber-glass fabric material behaves non-linearly in tension along wrap and weft direction and in-plane shear too [5].

2 Low-velocity impact test

The tested sandwich structure were made from 3 layers of fiber-glass fabric with the product name Aeroglass (390 g/m^2) and epoxy resin Epicote HGS LR 285. The composite laminate skins of total thickness 1.2 mm. The core was a close cell cross-linked polymer foam Airex C70.55. The wide sandwich beam of dimension 400 mm × 150 mm and overall thickness 12.5 mm was subjected to transverse low-velocity impact using drop-testing machine. The testing device enables to set the impact place on tested body and the height of impactor directly via moveable horizontal and vertical linear guides. The impactor of total weight 2.336 kg was equipped by force sensor (Kistler 9712B) that enables to record the time-force response (contact force) between the spherical head of impactor with radius 15 mm and tested body. Impacts were aimed at the centre of upper skin of tested sandwich beam. The response of sandwich structure was measured in form of deflection in three selected points simultaneously using the laser sensors. The sampling frequency of force sensor placed on head of impactor and all four laser sensor was the same, 20 kHz. The sandwich beams were simply supported on the steel stand along the shorter edges with the overlap 17.5 mm on the every side. The impact events were recorded using high-speed digital camera (Olympus i-Speed 2) with the frame rate 2000 fps. The geometry of tested sandwich beam together with the placement of selected measured points on upper skin of the beam is shown on Fig. 1.

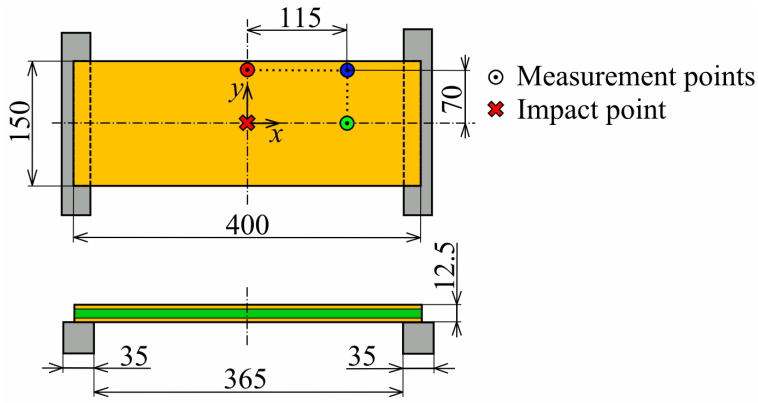

Fig. 1: Geometry of tested sandwich beam and the positions of measurement.

The range of impact velocities was varied between 2.0 and 5.0 $\mathrm{m \cdot s^{-1}}$. The impactor was accelerated only by the gravity. The real impact velocities of impactor on sandwich beam were affected by the friction in the linear guides of drop tool apparatus, therefore the real impact velocities of impactor were measured using the fourth laser sensor. The comparison between the impact velocities given by free fall of impactor and real impact velocities of impactor affected due to friction in the linear guides is summarized in Tab. 1.

Tab. 1: Comparison between theoretical and real impact velocities subjected to tested sandwich structure.

Impact velocity $[\mathrm{m \cdot s^{-1}}]$	Real impact velocity $[\mathrm{m \cdot s^{-1}}]$	Real impact energy [J]
2.00	1.89	4.17
3.00	2.91	9.89
4.00	3.92	17.95
4.50	4.39	22.51
5.00	4.83	27.25

Fig. 2 shows the process of impact event on wide sandwich beam captured by high-speed camera for impact velocity 5.0 $\mathrm{m \cdot s^{-1}}$. The foam crushing under the impactor starts at the time t = 2.5 ms after the begin of impact event (t = 0.0 s). The damage of the upper composite skin begin at the time t = 5.5 ms. This

damage propagates in form of crack across the upper skin - time t = 6.0 ms. The maximal deflection of the tested beam is achieved during the impact at the time t = 15.5 ms.

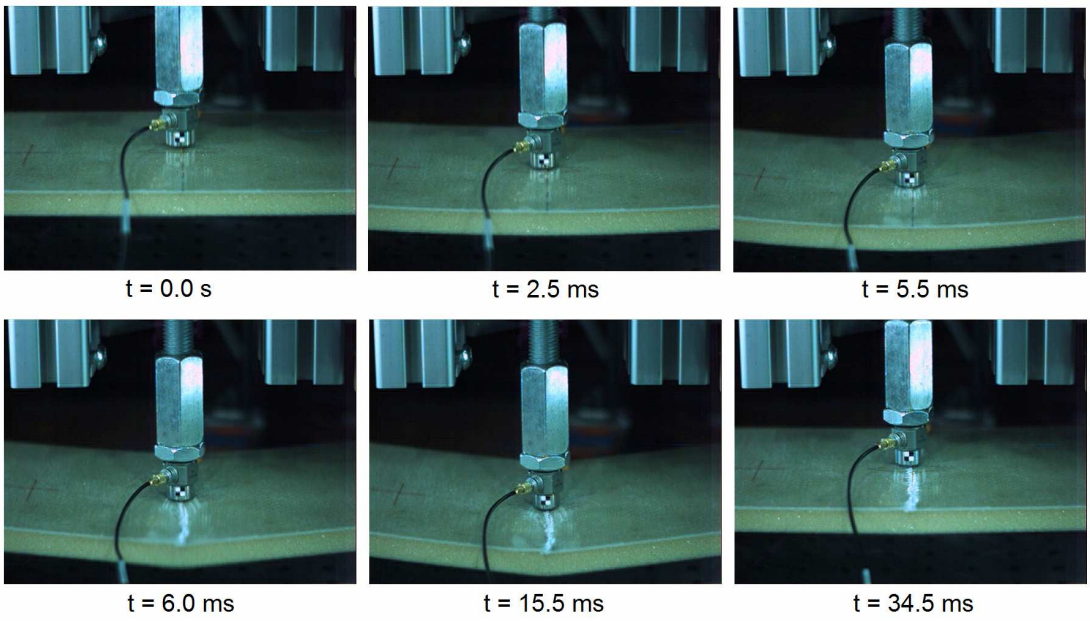

Fig. 2: Pictures of impact event on wide sandwich beam obtained high-speed camera for impact velocity 5.0 $\mathrm{m \cdot s^{-1}}$.

3 Material model and material parameters

3.1 Material model of composite skin

Sandwich composite fabric skin was modelled using a user defined orthotropic material model with the non-linear elastic behaviour. This material model was implemented into Abaqus software using VUMAT subroutine written in Fortran code. The transitions between linear and non-linear parts of stress-strain relationship are indicated using the values of deformations ε_{0i} (i = 1, 2) in principal directions 1 and 2 during loading. The non-linear function with the constant asymptote was considered in the case of the shear in plane 12 [6] Eq. (6). The resulting stress-strain relationship of laminated sandwich skin is described by following equations [7]

$$\sigma_1 = C_{11} \cdot \varepsilon_1 \cdot (1 - D_{11}) + C_{12} \cdot \varepsilon_2 \cdot (1 - D_{12}) + C_{13} \cdot \varepsilon_3 \cdot (1 - D_{13}), \text{ for } \varepsilon_1 < \varepsilon_{01}, \tag{1}$$

$$\sigma_1 = C_{11} \cdot \left[\varepsilon_1 + \frac{A_1}{2} \cdot \left(\varepsilon_{01}^2 - \varepsilon_1^{\,2} \right) - A_1 \cdot \varepsilon_{01} \cdot \left(\varepsilon_{01} - \varepsilon_1 \right) \right] \cdot (1 - D_{11}) + C_{12} \cdot \varepsilon_2 \cdot (1 - D_{12}) + \ldots \\ C_{13} \cdot \varepsilon_3 \cdot (1 - D_{13}), \quad \text{for } \varepsilon_1 \geq \varepsilon_{01} \tag{2}$$

$$\sigma_2 = C_{12} \cdot \varepsilon_1 \cdot (1 - D_{12}) + C_{22} \cdot \varepsilon_2 \cdot (1 - D_{22}) + C_{23} \cdot \varepsilon_3 \cdot (1 - D_{23}), \text{ for } \varepsilon_2 < \varepsilon_{02}, \tag{3}$$

$$\sigma_2 = C_{12} \cdot \varepsilon_1 \cdot (1 - D_{12}) + C_{22} \cdot \left[\varepsilon_2 + \frac{A_2}{2} \cdot \left(\varepsilon_{02}^2 - \varepsilon_2^{\,2} \right) - A_2 \cdot \varepsilon_{02} \cdot \left(\varepsilon_{02} - \varepsilon_2 \right) \right] \cdot (1 - D_{22}) + \ldots \\ C_{23} \cdot \varepsilon_3 \cdot (1 - D_{23}), \quad \text{for } \varepsilon_2 \geq \varepsilon_{02}, \tag{4}$$

$$\sigma_3 = C_{13} \cdot \varepsilon_1 \cdot (1 - D_{13}) + C_{23} \cdot \varepsilon_2 \cdot (1 - D_{23}) + C_{33} \cdot \varepsilon_3 \cdot (1 - D_{33}), \tag{5}$$

$$\tau_{23} = G_{23} \cdot \gamma_{23} \cdot (1 - D_{44}), \tag{6}$$

$$\tau_{13} = G_{13} \cdot \gamma_{13} \cdot (1 - D_{55}), \tag{7}$$

$$\tau_{12} = \frac{G_{12}^0 \cdot \gamma_{12}}{\left[1 + \left(\frac{G_{12}^0 \cdot |\gamma_{12}|}{\tau_{12}^0}\right)^{n_{12}}\right]^{\left(\frac{1}{n_{12}}\right)}} \cdot (1 - D_{66}), \tag{8}$$

$$\begin{aligned} C_{11} &= \frac{E_1 \cdot [1 - \nu_{23} \cdot \nu_{32}]}{\Delta}, \quad C_{12} = \frac{E_1 \cdot [\nu_{21} + \nu_{23} \cdot \nu_{32}]}{\Delta}, \quad C_{13} = \frac{E_1 \cdot [\nu_{31} + \nu_{32} \cdot \nu_{21}]}{\Delta}, \\ C_{22} &= \frac{E_2 \cdot [1 - \nu_{31} \cdot \nu_{13}]}{\Delta}, \quad C_{23} = \frac{E_2 \cdot [\nu_{32} + \nu_{31} \cdot \nu_{12}]}{\Delta}, \quad C_{33} = \frac{E_3 \cdot [1 - \nu_{12} \cdot \nu_{21}]}{\Delta}, \end{aligned} \tag{9}$$

where

$$\Delta = 1 - \nu_{12} \cdot \nu_{21} - \nu_{23} \cdot \nu_{32} - 2 \cdot \nu_{12} \cdot \nu_{23} \cdot \nu_{31}.$$

The material parameters E_1, E_2 and E_3 are Young's moduli in principal directions 1, 2 and 3; and ν_{12}, ν_{23}, ν_{31} Poisson's ratios in planes defined by principal directions 1, 2 and 3. Shear modulus in plane 23 and 13, is designated as G_{23} and G_{13}, respectively. The parameters A_1 and A_2 in Eq. (2) and (4) describe the straightening of yarns of fiber-glass fabric and the loss of stiffness in corresponding directions 1 and 2 respectively. The nonlinear behavior in case of shear in plane 12 (8) is described using initial shear modulus G_{12}^0, asymptotic value of shear stress τ_{12}^0 and shape parameter n_{12}.

The maximum stress failure criterion was used to predict failure on the composite skin

$$F_{1T} = \frac{\sigma_1}{X_T}, \quad F_{1C} = \frac{|\sigma_1|}{X_C}, \quad F_{2T} = \frac{\sigma_2}{Y_T}, \quad F_{2C} = \frac{|\sigma_2|}{Y_C}, \quad F_{12} = \frac{|\tau_{12}|}{S_L}, \tag{10}$$

where X and Y are the strengths in principal directions 1 and 2, the subscripts T and C denote tension and compression and S_L is the shear strength. The values of degradation variable D are dependent on the type of occurred failure. The degradation parameter in case of shear failure ($F_{12} \geq 1.0$) before the strain γ_{12} reaches the critical value of strain and $\gamma_{12} \geq \gamma_{12}^F$) was implemented from [8]. The degradation parameters are presented in different kinds of occurring failure in forms

$$\begin{aligned} &F_{1T} \geq 1 \Rightarrow D_{ij} = 1.0, \quad F_{2T} \geq 1 \Rightarrow D_{ij} = 1.0, \quad F_{12} \geq 1 \text{ and } \gamma_{12} \leq \gamma_{12}^F \Rightarrow D_{66} = 1 - e^{\left(\frac{1}{m_{12}} \cdot (F_{12})^{m_{12}}\right)}, \\ &F_{1C} \geq 1 \Rightarrow D_{11} = 0.6, \quad F_{2C} \geq 1 \Rightarrow D_{22} = 0.6, \quad F_{12} \geq 1 \text{ and } \gamma_{12} > \gamma_{12}^F \Rightarrow D_{ij} = 1.0. \end{aligned} \tag{11}$$

The non-negative constant m_{12} is presented by integer and γ_{12}^F is the ultimate deformation, when the material is fully damaged. The Fig. 3 shows the principle of linear and non-linear material behavior in principal direction 1 together with the principle of degradation in case of unaxial loading. The principle of non-linear function with constant asymptote in case shear plane 12 and applied material degradation is presented in Fig. 4.

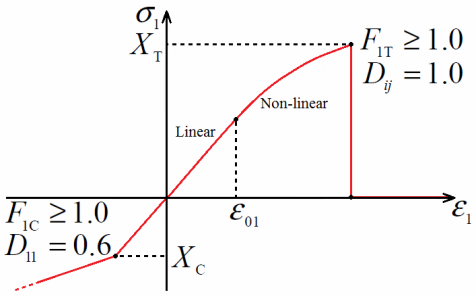

Fig. 3: The principle of linear and non-linear material behaviour together with material degradation in principal direction 1.

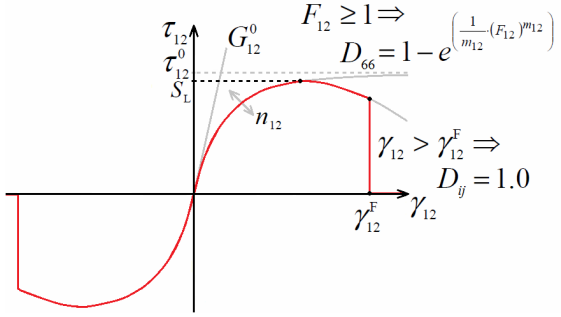

Fig. 4: The principle of material degradation of non-linear function with constant asymptote in plane 12.

Material parameters of considered material model of composite skin were identified from compressive and tensile tests using optimization process [7]. The material parameters E_3, G_{13} and G_{23} were taken from literature [9]. All material parameters of composite laminated skin of sandwich structure are summarized in Tab. 2.

Tab. 2: Material parameters of sandwich composite skin.

E_1	E_2	E_3	G_{13}	G_{23}	A_1	A_2	ε_{01}	ε_{02}	τ_{12}^0	m_{12}
[GPa]	[GPa]	[GPa]	[GPa]	[GPa]	[–]	[–]	[–]	[–]	[MPa]	[–]
16.9	18.5	8.0	4.0	2.75	10.0	14.0	0.0008	0.005	39.66	5

ν_{12}	ν_{23}	ν_{31}	ε_{12}^F	G_{13}^0	X_T	X_C	Y_T	Y_C	S_L	ρ_C
[–]	[–]	[–]	[–]	[GPa]	[MPa]	[MPa]	[MPa]	[MPa]	[MPa]	$[\mathrm{kg \cdot m^{-3}}]$
0.337	0.337	0.28	0.32	4.96	325	65	347	67	35	1154

3.2 Material model of foam core

Foam core of the sandwich structure was modeled using the Low Density Foam model [10]. This isotropic material model for highly compressible elastomeric foams assumes the zero Poisson's ratio. Material behavior was specified via defined unaxial stress-strain curves for tension and compression. The nonlinear elastic stress-strain behavior in tension was described via curve in form [7]

$$\sigma_i(\varepsilon_i) = 92.6 \cdot \ln(1+\varepsilon_i) + 198.8 \cdot [\ln(1+\varepsilon_i)]^2 - 134.2 \cdot [\ln(1+\varepsilon_i)]^3 - 2.3 \cdot [\ln(1+\varepsilon_i)]^4 + 11.8 \cdot [\ln(1+\varepsilon_i)]^5, \text{ where } i = 1, 2, 3. \quad (12)$$

The Fig. 5 shows the considered compressive and tensile stress-strain relationship of foam core of sandwich structure. The material is fully damaged after reaching the tensile strength R_{mT}. The compressive behaviour of the foam core was described as an ideally elastoplastic material. The compressive stress-strain curve has three distinct ranges. When the limit for linear-elastic compressive behaviour represented by compressive strength R_{mC} is reached, the foam core starts crushing at the same constant stress. When all cells of foam are crushed, the foam structure starts to respond as compacted foam. This state is in material model represented by ultimate compressive strain ε_U. The response of foam is characterised after reaching ε_U by sharp increase in stiffness. The material parameters of foam core are summarized in Tab. 4.

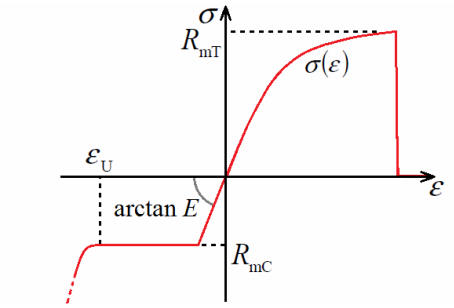

Fig. 5: Tensile and compressive stress-strain behaviour of foam core.

Tab. 4: Material parameters of sandwich foam core.

E	ν	R_{mT}	R_{mC}	ε_U	ρ_F
[MPa]	[–]	[MPa]	[MPa]	[–]	$[\mathrm{kg \cdot m^{-3}}]$
50.0	0.0	1.5	1.2	0.53	60.0

4 Numerical simulations and results

The numerical simulations were modeled in finite element software Abaqus 6.14 using explicit solver based on central difference scheme for time integration. The finite strain theory was assumed. The finite element model was created as a fully contact problem of four bodies. The friction between bodies has been neglected. 8-node solid elements (Type C3D8) were used. The finite element model of impactor was simplified and only the head of impactor was modeled with added mass to reach its real total weight. The real impact velocities form experiment were considered (see Tab. 1). The computed values of deflection were interpolated from displacements of neighbouring nodes of finite element mesh near the measure point of laser sensor from the experiment.

The results from experiment and numerical simulation represented by deflections in measuring points and by the time dependencies of the contact force were compared for the range of t = 0 – 20 ms from the start of impact event for impact velocities in range 2 – 4.5 $\mathrm{m \cdot s^{-1}}$. The damage area in form of spherical cap due to foam crushing was occurred for this impact velocities. The results comparison in case of impact velocity 5.0 $\mathrm{m \cdot s^{-1}}$ is performed for the range of time t = 0 – 40 ms due to occurrence of different kind of damage in form of rupture of outer composite skin. The detail of ruptured upper composite skin at the end of impact event is shown on Fig. 6, where are compared the damage from numerical simulation and the experiment. The damage in compression in principal direction 2 is shown in case of numerical simulation. The blue area corresponds to damage in tension in principal direction 1. The comparison of deflections and contact forces dependencies on the time is shown for selected impact velocities 3, 4 and 5 $\mathrm{m \cdot s^{-1}}$ on Fig. 7 – 9.

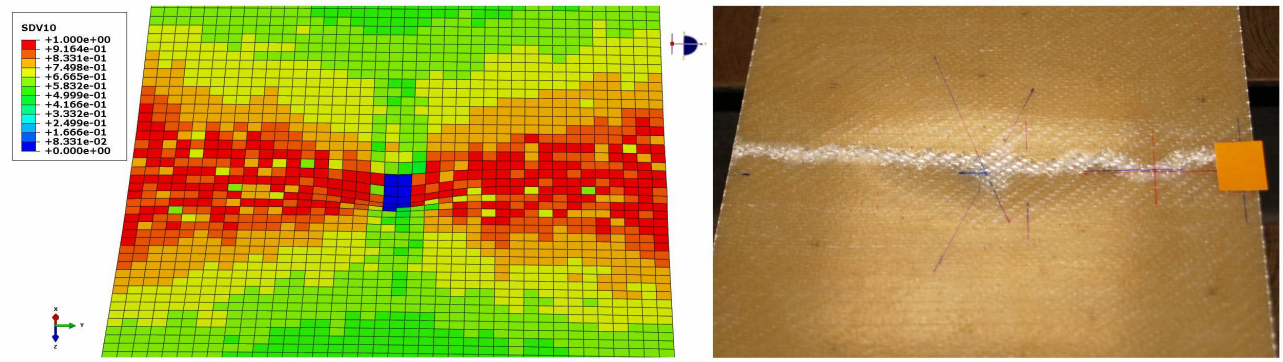

Fig. 6: The comparison of occurred damage on upper composite skin of sandwich beam from numerical simulation and experiment for impact velocity 5.0 $\mathrm{m \cdot s^{-1}}$.

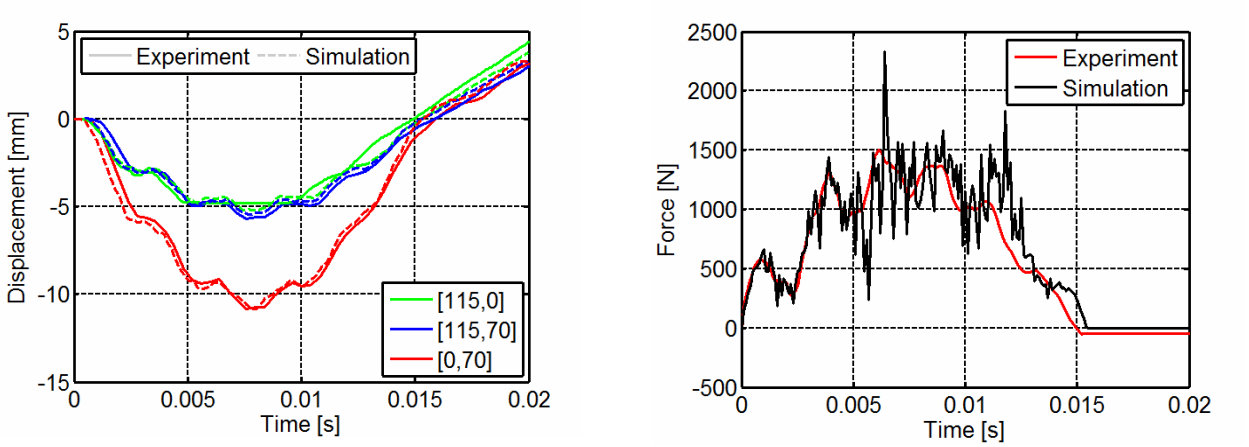

Fig. 7: Comparison of deflection (left) and contact force (right) of sandwich wide beam between numerical simulation and experiment for impact velocity 3.0 $\mathrm{m \cdot s^{-1}}$.

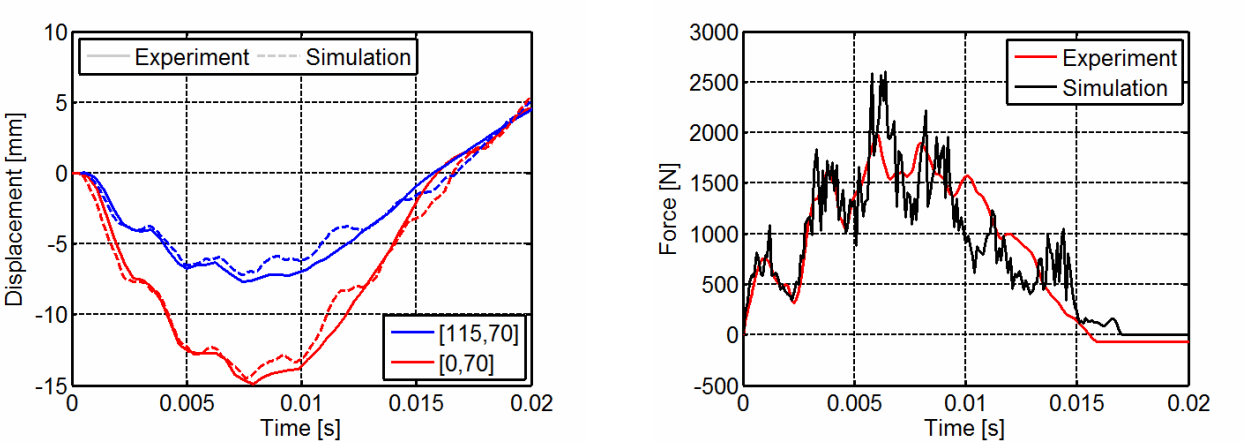

Fig. 8: Comparison of deflection (left) and contact force (right) of sandwich wide beam between numerical simulation and experiment for impact velocity 4.0 $\mathrm{m \cdot s^{-1}}$.

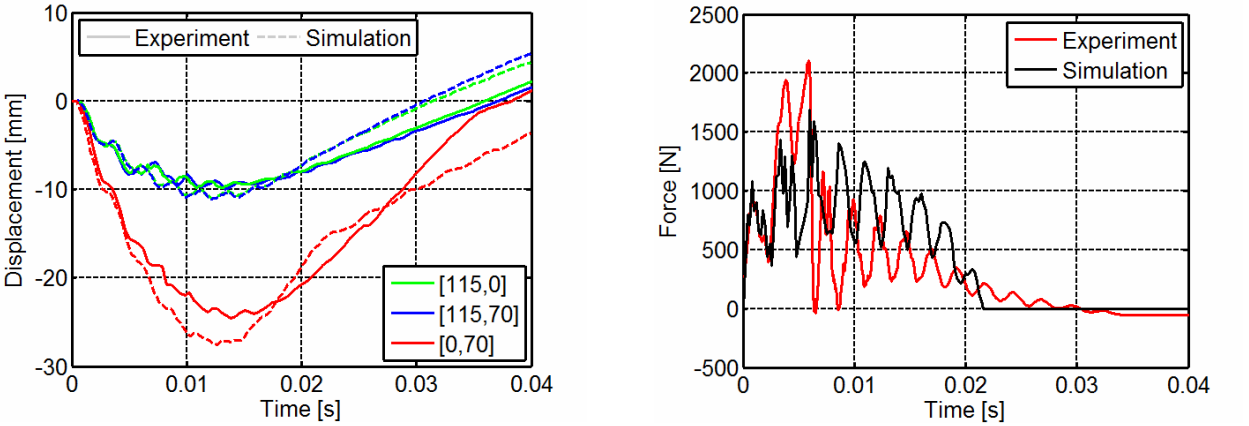

Fig. 9: Comparison of deflection (left) and contact force (right) of sandwich wide beam between numerical simulation and experiment for impact velocity 5.0 $\mathrm{m \cdot s^{-1}}$.

5 Conclusion

The response of composite beam to low-velocity impact has been investigated experimentally and numerically. The experimental results in form of deflection and contact force time dependencies were compared with results from numerical model for all performed impact velocities. The results of contact force time dependencies do not show perfect agreement in form of occurrence of the peaks in case of numerical simulations, because the damping of contact between impactor and upper skin was neglected. The damage was compared only by the visual inspection with the resultant damage from the numerical simulations. The expected occurrence of tensile failure of lower composite skin during the impact did not occurred in case of experiment and numerical simulation too. The delamination between the skins and the foam core did not occurred in case of experimental testing, therefore thus behavior is not included in the material model because of reasonable time consumption of numerical analysis. Generally, sufficient agreement between experiments and numerical simulations was achieved.

Acknowledgement

T. Mandys, T. Kroupa and V. Laš were supported by the project LO1506 of the Czech Ministry of Education, Youth and Sports, J. Bartošek was supported by the student research project of Ministry of Education of Czech Republic No. SGS-2016-038 and C. Štádler was supported by the student research project of the Ministry of Education of the Czech Republic No. SGS-2014-022.

References

[1] Wang J., Waas A. M., Wang H., Experimental and numerical study on the low-velocity impact behavior of foam-core sandwich panels, Composite Structures (2013) vol. 96, pp. 298-311.

[2] Sadílek P., Zemčík R., Bartošek J., Mandys T., Active structural health monitoring of composite plates and sandwiches, Applied and Computional Mechanics (2013), vol. 7, pp. 183-192.

[3] Zemčík R., Laš V., Kroupa T., Bartošek J., Reconstruction of Impact on Textile Composite Plate Using Piezoelectric Sensors, Proceedings of the Ninth International Workshop on Structural Health Monitoring (2013), Stanford University, Stanford, Vol 1, pp. 393-400.

[4] Kroupa T., Krystek J., Srbová H., Janda P., Plastic behavior in shear and degradation of shear modulus of textile composite materials with simple plane wave, Experimental Stress Analysis 2011, Brno University of Technology, Brno, pp. 169-176.

[5] Kunc K., Kroupa T., Zemčík R., Krystek J., Tensile and compressive tests of textile composites and its result analysis, 22st. international conference on materials and technology, Program and book of abstracts (2014), Ljubljana, pp. 134-134.

[6] Kroupa T., Zemčík R., Klepáček J., Temperature dependence of parameters of non-linear stress-strain relationship for carbon epoxy composites, Materials and Technology (2009), vol. 43, no. 2, pp.69-72.

[7] Mandys T., Kroupa T., Laš V., Progressive failure analysis of composite sandwich beam in case of quasistatic loading, Materials and technology (2014), vol. 48, no. 4, pp. 593-597.

[8] Yen C. F., Ballistic Impact modeling of composite materials, 7th International LS-Dyna User's Conference (2006), Dearborn, Michigan.

[9] Zemčík R., Laš V., Kroupa T., Purš H., Identification of material characteristics of sandwich panels, Bulletin of Applied Mechanics (2011), vol. 26, pp. 26–30.

[10] Abaqus 6.14 Documentation, Dassault Systèmes Simulia Corp., 2014.